EARTHQUAKE ENGINEERING AND STRUCTURAL DYNAMICS, VOL. 19, 1089–1106 (1990)

A STRONG MOTION DATABASE FOR THE CHIBA SEISMOMETER ARRAY AND ITS ENGINEERING ANALYSIS

TSUNEO KATAYAMA, FUMIO YAMAZAKI, SHIGERU NAGATA, LIN LU AND TURGAY TURKER

Institute of Industrial Science, University of Tokyo, 7-22-1 Roppongi, Minato-ku, Tokyo 106, Japan

SUMMARY

A three-dimensional seismometer array was installed in the Chiba Experiment Station of the Institute of Industrial Science, University of Tokyo in 1982. The array system consists of 44 three-component accelerometers densely placed both on the ground surface and in boreholes. A complementary system for the measurement of ground and buried pipe strains was also installed at the same site. The array system has been successfully in operation, and more than 160 earthquakes have been recorded. Considering a wide use of these seismograms, the Chiba array database has recently been created comprising twenty-seven major events. This paper describes the Chiba array system and its strong motion database. Results of engineering analysis using the selected records are also presented.

INTRODUCTION

Array observation is one of the powerful tools to investigate various characteristics of earthquake ground motions. Depending on the aim of observation, there are several ways in which the seismometers may be arranged. One of the typical types is a two-dimensional surface array such as SMART-1[1,2] in Taiwan which has three concentric circles with radii of 200 m, 1 km and 2 km. The records from this array have been utilized by a number of researchers[3–6] to study the propagation and spatial variation of seismic waves. There are also a number of one-dimensional vertical arrays[7–9] for the investigation of soil amplification and non-linear response. The use of records from these arrays, however, is limited to the array owners in most cases.

A unique array system[10–13] was installed in the Chiba Experiment Station of the Institute of Industrial Science, University of Tokyo in 1982. In this array, seismometers are placed very densely both on the ground surface and in boreholes, thus constituting a three-dimensional network. Hence the records obtained from the array may be particularly useful for evaluating the spatial correlation of earthquake ground motions over a short separation distance and for examining the amplification theory. Note that there are some other three-dimensional dense arrays recently installed; e.g., one in Lotung, Taiwan[14] to investigate soil–structure interaction, one in Tokyo International Airport (Haneda[15]) to study soft soil behaviour during earthquakes, and four sites around the Suruga Bay-Izu region[16] to investigate the effect of geological and topographical conditions on earthquake ground motions.

The Chiba array has been successfully in operation and more than 160 events have been recorded. In order to utilize these records effectively, a strong motion database consisting of twenty-seven major events is created. Although many earthquake ground motions have been obtained by a number of array systems, no common database exists in Japan. In the United States, however, World Data Center A for Solid Earth Geophysics, National Oceanic and Atmospheric Administration (NOAA), collects, archives and disseminates strong motion records[17] as well as other engineering data. Recently the Earthquake Engineering Committee of the Japan Society of Civil Engineers (JSCE) advocated the development of a cooperative database system in Japan.[18] The authors are willing to provide the Chiba array records when such a system is established.

0098–8847/90/081089–18$09.00

Received 18 April 1990
Revised 18 July 1990

DENSE SEISMOMETER ARRAY IN CHIBA STATION

Site condition

The Chiba Experiment Station is located about 30 km east of Tokyo. The longitude of the station is 140° 6′37″E and the latitude is 35° 37′17″N. Figure 1 shows the layout of boreholes where the standard penetration tests were carried out. The topographical and geological conditions of the site are generally simple with the ground surface being almost flat.

Figure 2 shows the soil profiles at seven boreholes (C0 and P5–P0) in the Chiba Station. The top 3–5 m of the site is loam having standard penetration *N* values less than 10. The loam layer is underlain by a sandy clay layer of thickness 2–4 m having *N* values also less than 10. A diluvium sand layer lies under the clay layer and its *N* values are greater than 20–30. This sand layer, whose stiffness increases with depth, is interspersed with clayey layers having relatively small *N* values. In spite of slight differences in the depths of boundaries between different layers from one borehole to another, the layering is quite uniform, indicating a relatively simple soil profile. The groundwater table was found to be lower than GL − 5 m. In the borehole C0, the elastic wave velocities were measured by downhole shooting, giving the results shown in Figure 2.

Dense array system

A dense array observation began within the Chiba Experiment Station in April, 1982. Near the ground surface (GL − 1 m), accelerometers are placed in the boreholes shown in Figure 1. At that time, the array system was composed of eleven boreholes (C0–C4 and P1–P6) with thirty-six accelerometers. Four boreholes (P7–P0) with eight accelerometers were added to the array in January, 1985. The numbers and locations of borehole accelerometers are listed in Table I.

There is a large triangular network P0–P8–P5 with each of the three sides being approximately 300 m. Around borehole C0, eight accelerometers are densely arranged. Four of them (C1–C4) are only 5 m from C0, and the other four (P1–P4) are 15 m from C0. The large triangular network was laid to obtain the macroscopic propagation properties of seismic waves, while the very densely located array was established primarily to investigate the local soil strain characteristics during earthquakes. Although there are several low-storied buildings and research facilities in the Chiba Station, they are located not so close to the boreholes. Thus recorded ground motions can be considered free-field ones.

Piezoelectric type acceleration transducers are used for the array observation. These accelerometers have a nearly flat sensitivity in the frequency range between 0·1 and and 30 Hz. Three transducers (two horizontal and one vertical) and their amplifiers were installed in a cylindrical steel casing with an external diameter of 65 mm and a length of 335 mm. The accelerometers were then installed in boreholes with diameters of 116 mm. A maximum of five accelerometers was to be installed at different depths in a single hole. The accelerometers were fixed at predetermined depths by using cement mortar.

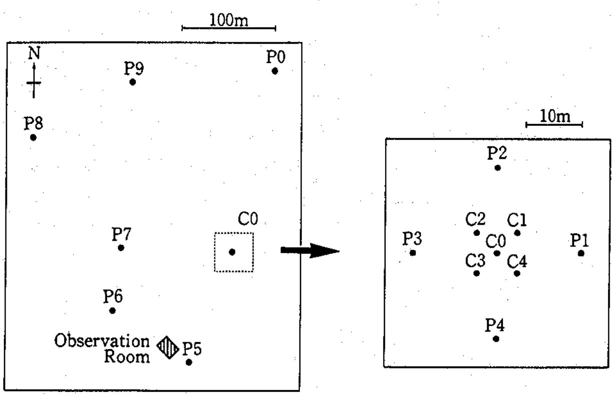

Figure 1. Layout of boreholes in the Chiba array

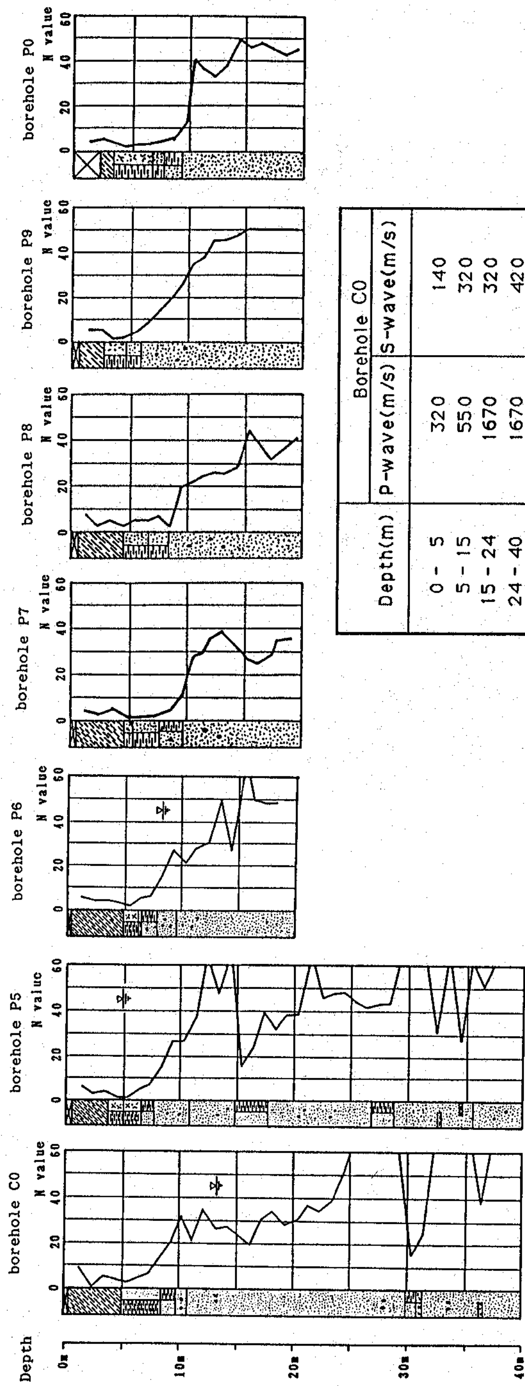

Borehole C0		
Depth(m)	P-wave(m/s)	S-wave(m/s)
0 - 5	320	140
5 - 15	550	320
15 - 24	1670	320
24 - 40	1670	420

Figure 2. Soil profiles of Chiba Experiment Station

Table I. Location of borehole accelerometers in the Chiba array

Depth (m)	Borehole														
	C0	C1	C2	C3	C4	P1	P2	P3	P4	P5	P6	P7	P8	P9	P0
1	○	○	○	○	○	○	○	○	○	○	○	○	○	○	○
5	○	○	○	○	○										
10	○	○	○	○	○	○	○	○	○	○	○				
20	○					○	○	○	○	○	○	○	○	○	○
40	○									○					

In December 1984, an additional system, which consists of simultaneous measurements of acceleration, velocity and displacement, was introduced on the ground floor of the building where recording units are located. The velocity seismograph developed by Muramatsu[19] and the low-magnification displacement seismograph of the Japan Meteorological Agency (JMA) are employed along with the piezoelectric accelerometer.

Complementary measurement system

In addition to the accelerometer array network, a complementary measurement system was also installed in June, 1983. This system consists of buried pipes of two different materials and three ground strain gauges as depicted in Figure 3. A welded steel pipe and a ductile-cast-iron pipe of diameter 150 mm are buried at GL − 1·3 m. Twenty-nine strain gauges were attached to these pipes to measure the strain in the steel pipe (denoted by 'SS#' in Figure 3), the strain in the ductile-cast-iron pipe (DS#) and the relative displacement over the joint in the ductile-cast-iron pipe (DJ#).

The relative displacements of the ground are directly measured at GL − 1·3 m by means of three displacement transducers, G1–G3, shown in Figure 3. The instrument consists of two 9 mm-thick discs with a diameter of 80 cm and a double tube connecting them at a distance of 3 m. The transducer is placed in the external pipe and it measures the relative displacement between the discs. Note that all the measured relative displacements are converted to strains in the strong motion database.

Recording system

The signals from all the seismometers and strain gauges are recorded at every 0·005 s by three 64-channel digital recorder units. The system is always kept in a full operational status. The signals are continuously fed into the storage which is capable of keeping the most recent 1·5 s signals. The recording devices are activated when any one of the three components at P540 (GL − 40 m in the borehole P5) exceeds 1·0 cm/s^2. The system continues in operation for 30 s after the motion falls below this trigger threshold level. Each recorder has a digital magnetic tape with a recording capacity of 30 min. Timing information is internally generated, and in addition, the absolute time is corrected hourly by utilizing the signal from NHK radio station.

DEVELOPMENT OF CHIBA ARRAY DATABASE

Selection of earthquakes

In the Chiba array, more than 160 earthquakes have been recorded since 1982 with about 15 000 acceleration, strain and velocity components. Since the trigger is set at a relatively low level, most of the events are small ones. Thus we selected only major earthquakes for the Chiba array database. Twenty-seven events whose peak ground acceleration at C001 (GL − 1 m in the borehole C0) is larger than 20 cm/s^2 or whose maximum steel pipe strains (SS1–SS3) are larger than 5×10^{-6} are selected.

Table II summarizes the basic information on these events at the Chiba array. The epicentres of these events are plotted in Figure 4. The largest event in the database is the Chibaken-Toho-Oki earthquake of

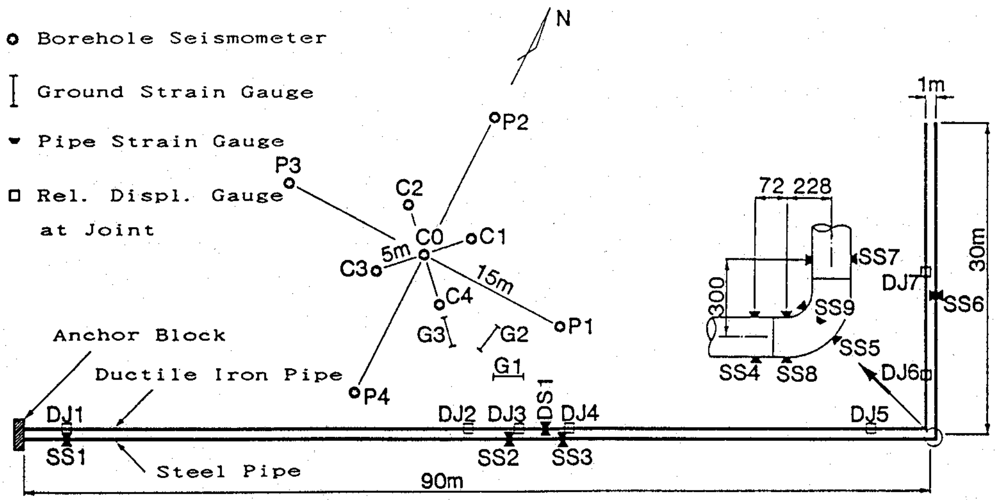

Figure 3. Layout of complementary observation system of the Chiba array

December 17, 1987 with the peak ground acceleration over 300 cm/s^2 at ground surface and the maximum buried pipe strain over 5×10^{-5}. All the other events are much smaller than this Chibaken-Toho-Oki event.

Development of database

The procedure of the database construction is shown in Figure 5. The voltage signals from the seismometers and strain gauges are stored on digital magnetic tapes. Multiplying the conversion factor to these voltage values, the real values for the acceleration, velocity and strain are obtained. The baseline correction is also carried out in this stage to have zero-mean for acceleration and velocity records. For strain records, zero-mean is assumed only for the initial delay time (= 1·5 s) since they sometimes exhibit a shift of baseline owing to the friction of joints. A slight time lag of input signals among three records was found to occur, and it may have a different value for a different event. Thus the time lag correction is performed by comparing the same signals in the three recorders.

After judging whether or not an event is large enough for the criterion described previously, its duration to be used for the database is determined. Because the duration is sometimes too long for a whole record to be stored in the database, the record is truncated at the time when the cumulative power of horizontal acceleration records at C001 exceeds 99 per cent of that for the total recording time. By checking the arrival of the P-wave at P540, the initial zero part of record within the delay time is also reduced to be about 0·5 s when determining the duration.

After these operations, the strain and velocity records are stored in the database. However, further corrections are applied to the acceleration records. Considering the sensitivity of the accelerometer, a high-cut filter is employed to remove possible noise. Following a cosine curve, the Fourier amplitude of the records is reduced to be zero between 27 and 33 Hz. Note that this filtering has only a small effect on the records.

At the early stage of the array installation, an orientation error of the buried accelerometers was detected.[10] Because of the cylindrical shape of the casing and its small resistance against rotation, most of the accelerometers rotated about their vertical axes during installation. The rotation of accelerometers about their two horizontal axes might also occur although these rotation angles were limited by the space in each borehole. When constructing the database, a detailed study for the three-dimensional correction of orientation error has been carried out using the recorded ground motions. The rotation angles to restore the correct directivity were then determined by the maximum cross correlation method. Note that, in the course of this study, we also found orientation errors in some other array systems. A separate paper on this topic is now in preparation. After all these corrections, the acceleration database was completed.

Table II. Basic information on earthquake records in Chiba array database

No.	IEQK	Trigger time at P540		Focal depth (km)	JMA magnitude	Azimuth (deg.)	Epicentral distance (km)	Max. acceleration at C001 (cm/s^2)			Max. pipe strain ($\times 10^{-6}$)	T_D/T_R (s)
								EW	NS	UD		
1	8205	82· 7·23	23:24:30	30	7·0	68·9	178	28·3	26·1	11·7	—	216/322
2	8307	83· 2·27	21:14:33	72	6·0	6·6	35	47·4	55·7	13·2	15·7	80/182
3	8401	84· 1·01	18:04:47	388	7·3	234·4	373	25·5	24·2	12·7	6·9	141/223
4	8406	84· 3·06	11:19:03	452	7·9	187·2	702	22·3	28·0	7·8	11·1	281/347
5	8414	84· 9·14	8:49:33	2	6·8	276·3	232	3·3	4·5	1·8	18·8	281/307
6	8416	84· 9·19	2:03:32	13	6·6	142·5	219	13·8	14·5	7·8	5·1	181/216
7	8420	84·12·17	23:49:59	78	4·9	240·1	5	22·1	24·1	40·8	6·7	37/ 63
8	8510	85· 6·08	1:29:11	64	4·8	126·1	16	27·4	29·6	12·6	5·5	39/ 64
9	8519	85·10·04	21:26:05	78	6·1	9·0	28	59·2	82·2	23·5	18·2	55/156
10	8525	85·11·06	0:31:00	63	5·0	158·2	32	75·7	71·6	28·3	14·7	35/ 80
11	8601	86· 2·12	11:59:58	44	6·1	44·5	125	15·4	14·3	5·2	4·3	98/140
12	8602	86· 6·24	11:53:29	73	6·5	147·7	105	54·0	40·7	21·5	15·3	229/245
13	8611	86·11·22	9:42:14	15	6·0	204·3	131	5·2	6·0	2·7	19·5	185/199
14	8706	87· 2·06	22:17:00	35	6·7	46·7	219	11·3	14·0	6·3	10·2	170/218
15	8717	87· 6·30	18:17:21	57	4·9	358·2	62	20·7	33·5	12·1	4·8	43/ 68
16	8722	87·12·17	11:08:27	58	6·7	128·1	45	213·6	327·1	124·8	55·6	39/282
17	8723	87·12·17	11:15:14	52	4·6	128·2	46	17·2	21·2	16·4	6·4	51/ 64
18	8725	87·12·17	14:07:18	58	4·4	126·5	42	23·8	13·8	9·3	3·9	28/ 44
19	8726	87·12·17	15:30:07	42	4·0	128·8	52	22·5	30·4	18·0	5·6	24/ 39
20	8802	88· 1·05	10:09:17	42	4·2	128·3	37	40·6	40·8	10·1	7·8	17/ 39
21	8806	88· 1·16	20:42:20	48	5·2	133·3	38	54·9	97·8	19·8	15·9	37/ 81
22	8808	88· 1·18	19:37:24	32	4·1	243·6	17	19·0	26·2	9·6	4·4	19/ 34
23	8816	88· 3·18	5:34:45	96	6·0	276·3	42	48·4	59·8	15·2	18·3	59/138
24	8823	88· 8·12	14:15:08	69	5·3	200·8	62	46·4	35·2	12·0	11·6	44/ 70
25	8901	89· 2·19	21:27:21	55	5·6	337·6	48	55·7	49·1	25·4	12·8	54/118
26	8903	89· 3·06	23:39:56	56	6·0	81·5	55	27·5	28·9	13·2	9·4	81/141
27	8904	89· 3·11	16:12:33	45	4·9	52·0	52	41·0	21·9	15·3	6·5	29/ 51

T_D: duration for database.
T_R: duration of original record.
Azimuth: clockwise from north.

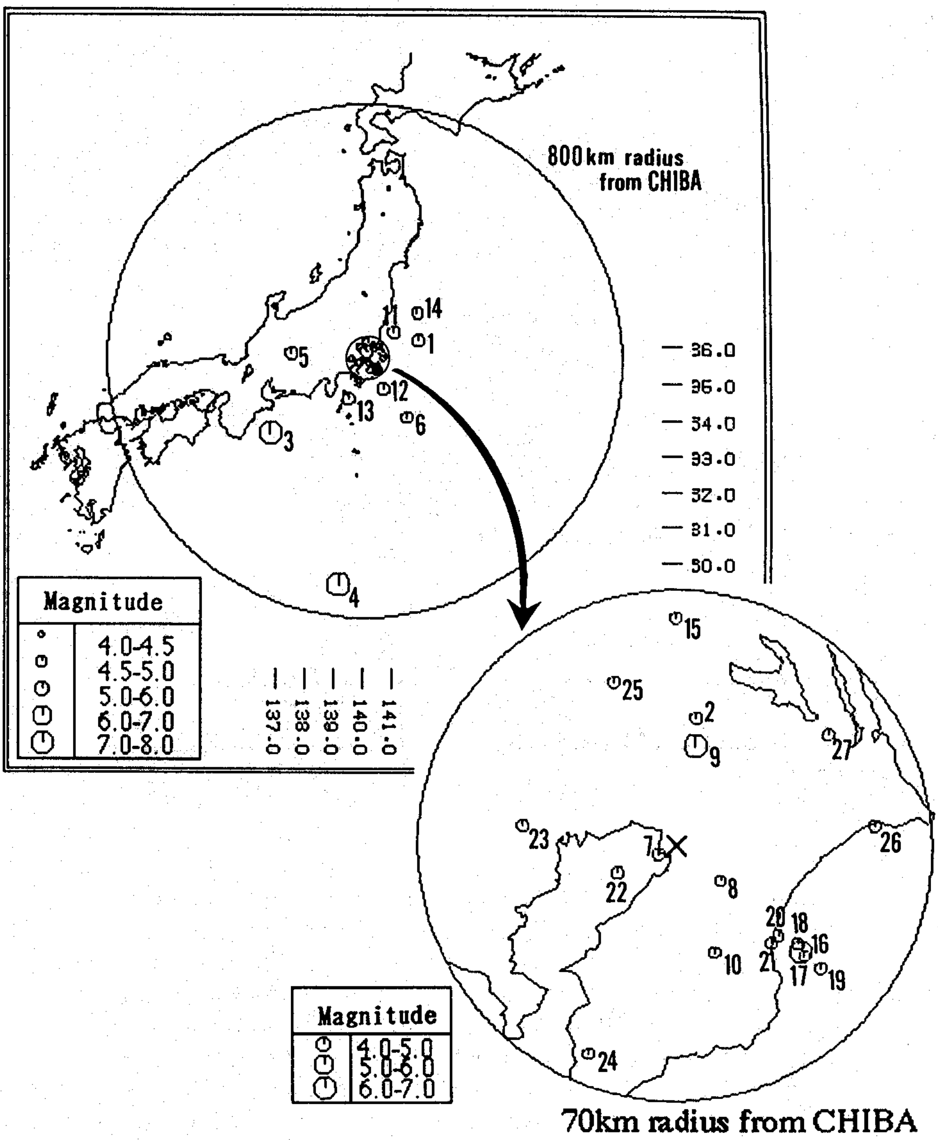

Figure 4. Epicentres of events in Chiba array database

Organization of database

These two databases, one for acceleration and one for strain and velocity, are stored in magnetic tapes by the EBCDIC code. Each database consists of 27 sequential datasets corresponding to the 27 events. Each dataset includes 135 records for the acceleration database and 37 records for the strain and velocity database. Each record is composed of heading data and time history data. The heading data include the event code (IEQK in Table II), the component code, the title of the record, the maximum value of the record, the time interval and the number of time steps. The time history data follow the heading data.

SPATIAL VARIATION OF GROUND MOTIONS DURING THE TOKYO-TOBU EARTHQUAKE

The Tokyo-Tobu earthquake (IEQE = 8816), which occurred in the eastern region (= Tobu) of Tokyo on March 18, 1988, was selected for the demonstration of the Chiba array database. Considering the direction of

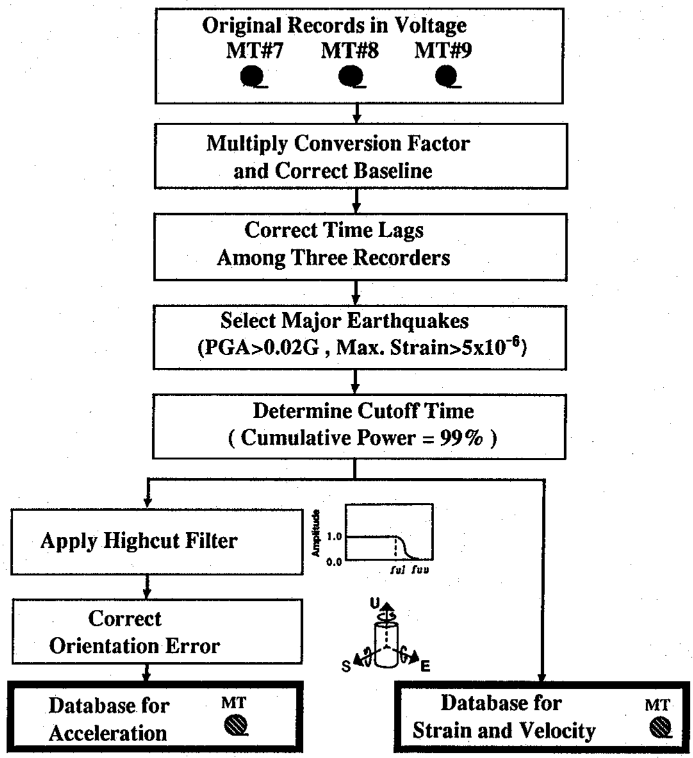

Figure 5. Procedure for construction of Chiba array database

epicentre, the radial components (S83·7° E) and transverse components (S6·3° W) were obtained from the original acceleration records. The acceleration time histories at C001 are shown in Figure 6 along with their Fourier spectra. Using a rectangular frequency window with a cosine taper, the orbit spectra of these records were calculated. Figure 7 shows the orbit spectrum for the radial and transverse components, and it indicates a dominance of the SH-wave in $f = 3{\cdot}2\text{–}4{\cdot}2$ Hz and that of the SV-wave in $f = 4{\cdot}8\text{–}5{\cdot}8$ Hz for the time window of 12–16 s. These facts can also be observed in the Fourier spectra.

Using the accelerogram recorded at 15 locations of GL − 1 m, the principal axes[20,21] were calculated for the time window of 12–16 s. The horizontal plane plots of the major and intermediate principal axes are shown in Figure 8 for the frequency windows of 3·2–4·2 and 4·8–5·8 Hz. In the figure, the coordinates of the accelerometers, the directions of the major principal axes and the variances of three principal axes are also listed. Note that, in this time window, the minor principal axis of each point was very close to the UD-direction. It is observed that the dominant direction and variance of the filtered waves at 15 locations were close to each other in these frequency ranges. However, they were highly scattered in the higher frequency range, and significant differences were observed even for 2 points only 15 m apart.

The spatial variation of earthquake ground motion is further examined with the aid of the coherence function

$$\mathrm{coh}^2(f) = \frac{|S_{xy}(f)|^2}{S_{xx}(f)S_{yy}(f)} \tag{1}$$

where S_{xx} and S_{yy} are the power spectra and S_{xy} is the cross spectrum. The Parzen window is employed in calculating these spectra with a bandwidth of 0·4 Hz. The coherence functions for six separation distances (5, 15, 30, 100, 157, 270 m) are shown in Figure 9. For the separation of 5 m, the coherence is very high and close to 1·0 up to 5–6 Hz. However, the higher frequency contents are incoherent even at a distance of 5 m. The

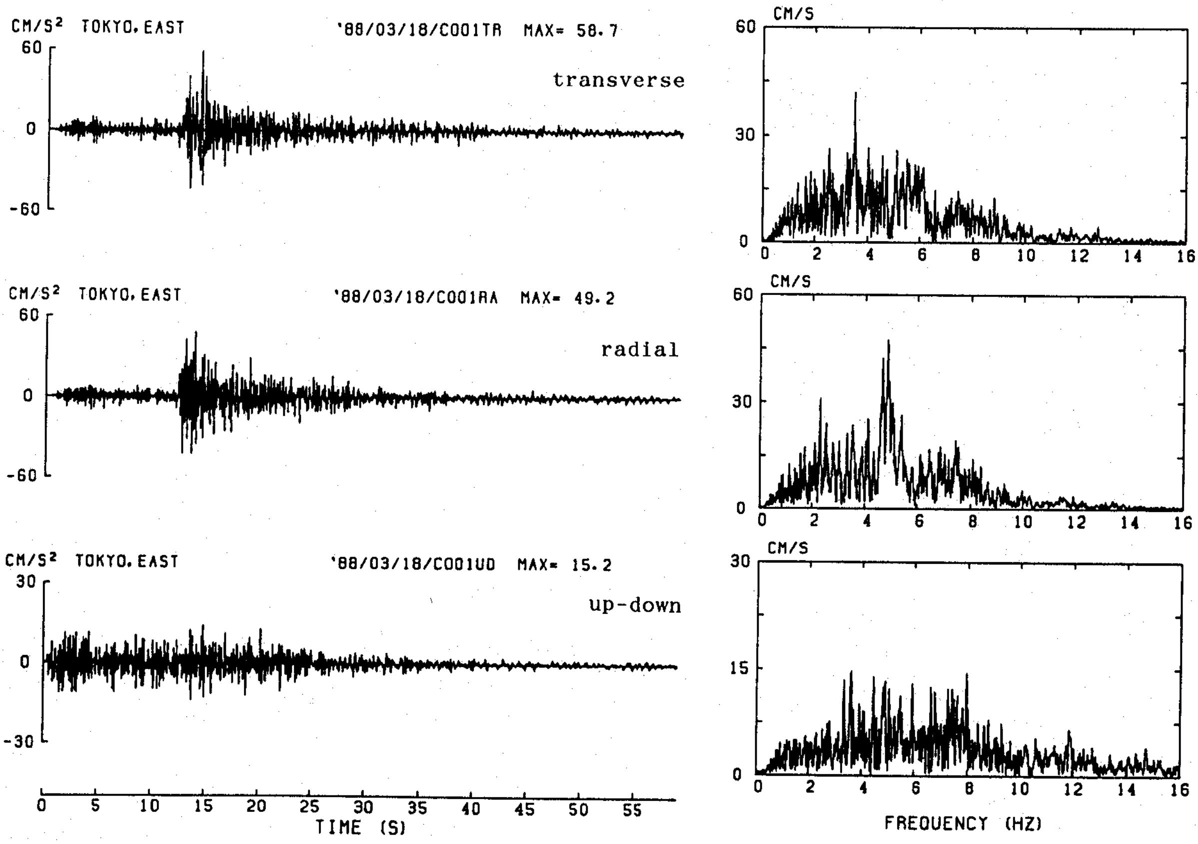

Figure 6. Acceleration time histories and their Fourier spectra for the Tokyo-Tobu earthquake at C001 point

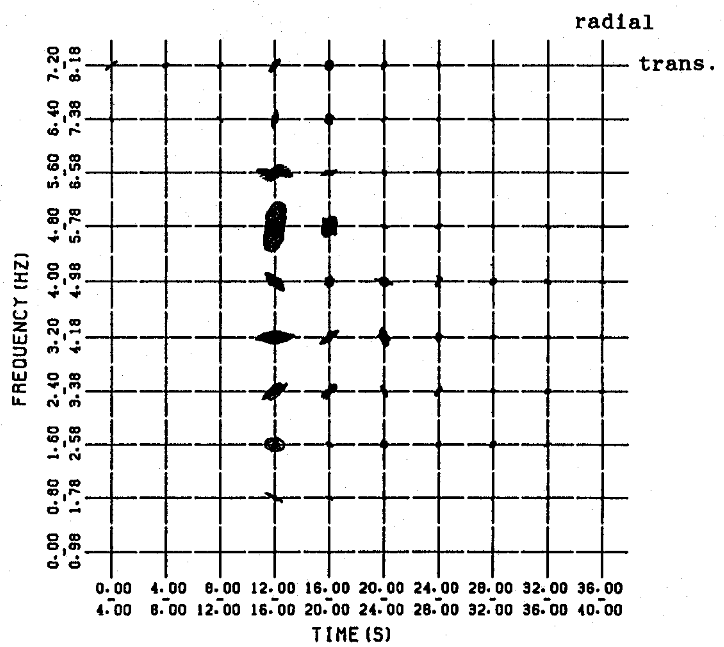

Figure 7. Orbit spectrum of the Tokyo-Tobu earthquake at C001 point for radial and transverse components

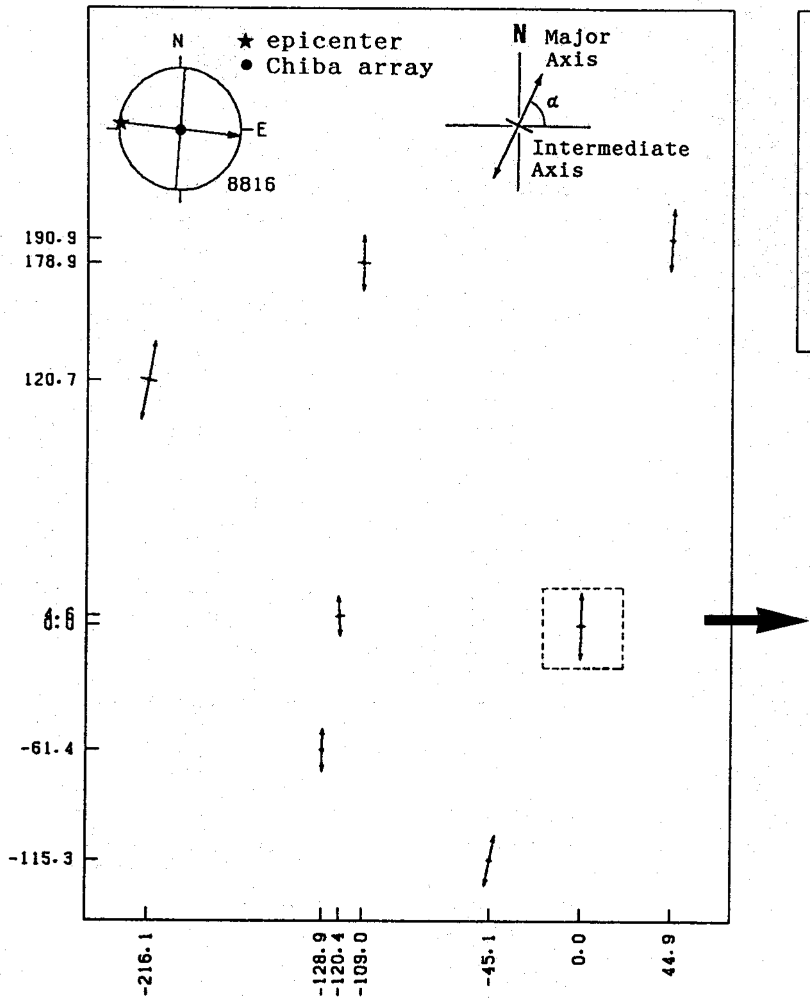

POINTS	X	Y	ALPHA	MAJOR	INTER	MINOR
C0	0.00	0.00	89.3	63.0	7.2	1.80
C1	3.54	3.54	85.0	60.3	6.6	1.46
C2	-3.54	3.54	86.4	73.7	9.9	1.57
C3	-3.54	-3.54	-88.3	69.4	10.1	1.51
C4	3.54	-3.54	89.5	63.6	6.4	2.37
P1	15.00	0.00	83.3	52.2	7.5	1.82
P2	0.00	15.00	78.8	69.3	15.4	1.04
P3	-15.00	0.00	-88.9	80.8	17.7	0.76
P4	0.00	-15.00	-85.5	68.1	9.5	1.92
P5	-45.13	-115.38	78.8	48.2	5.2	1.47
P6	-128.92	-61.42	89.5	40.3	3.7	1.16
P7	-120.43	4.67	-87.7	38.6	8.1	1.12
P8	-216.13	120.73	80.1	75.6	14.5	0.63
P9	-109.01	178.94	89.3	53.1	10.8	0.34
P0	44.94	190.90	86.8	59.3	5.4	1.71

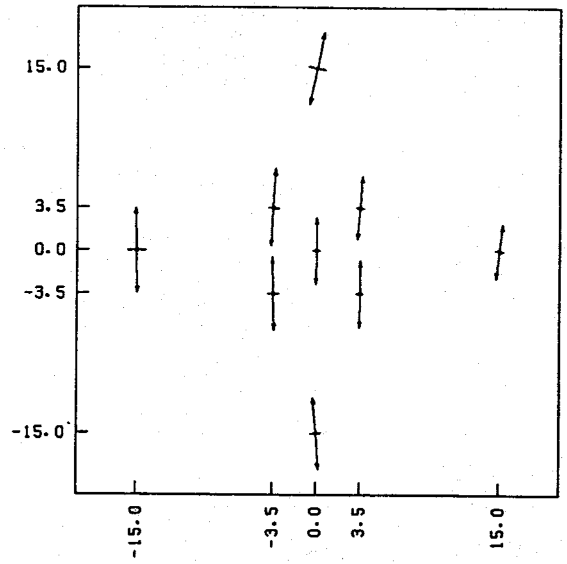

(a) f= 3.2 - 4.2Hz, t= 12 - 16s

Figure 8(a)

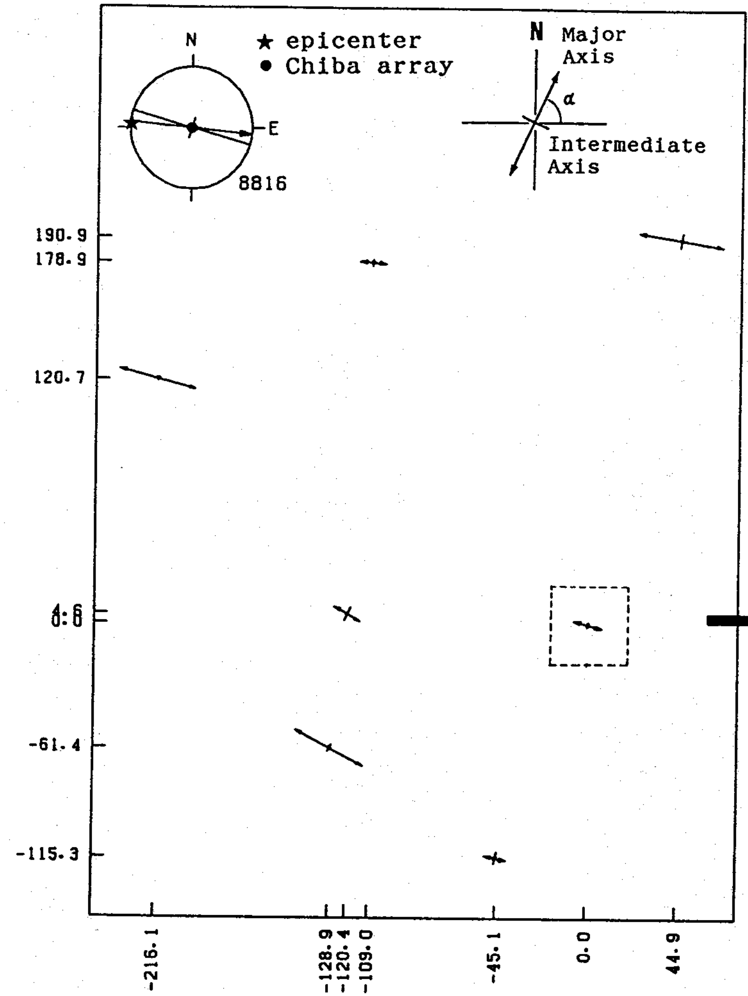

POINTS	X	Y	ALPHA	MAJOR	INTER	MINOR
C0	0.00	0.00	-15.9	121.5	23.5	3.83
C1	3.54	3.54	-18.6	111.9	22.6	2.95
C2	-3.54	3.54	-22.7	143.9	24.4	4.59
C3	-3.54	-3.54	-11.9	143.3	29.8	5.68
C4	3.54	-3.54	-9.9	147.2	28.7	3.31
P1	15.00	0.00	-15.6	125.1	29.7	4.55
P2	0.00	15.00	-15.4	246.1	17.2	2.36
P3	-15.00	0.00	-35.6	185.8	33.0	7.21
P4	0.00	-15.00	-3.9	157.8	19.4	6.26
P5	-45.13	-115.38	-11.9	90.4	50.6	22.36
P6	-128.92	-61.42	-27.4	325.6	31.4	2.78
P7	-120.43	4.67	-29.6	127.2	61.6	8.24
P8	-216.13	120.73	-14.7	328.2	14.6	11.89
P9	-109.01	178.94	-5.4	110.1	25.9	2.62
P0	44.94	190.90	-9.8	360.4	63.0	1.20

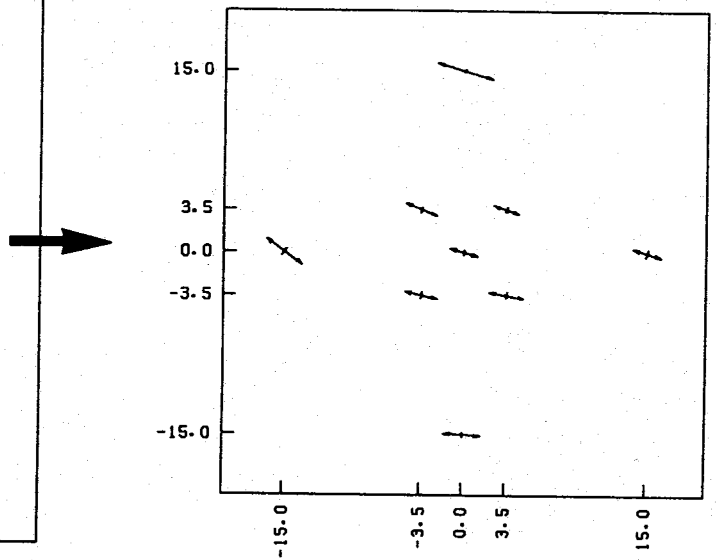

(b) f= 4.8 - 5.8Hz, t= 12 - 16s

Figure 8. Distribution of principal axes for filtered waves of the Tokyo-Tobu earthquake

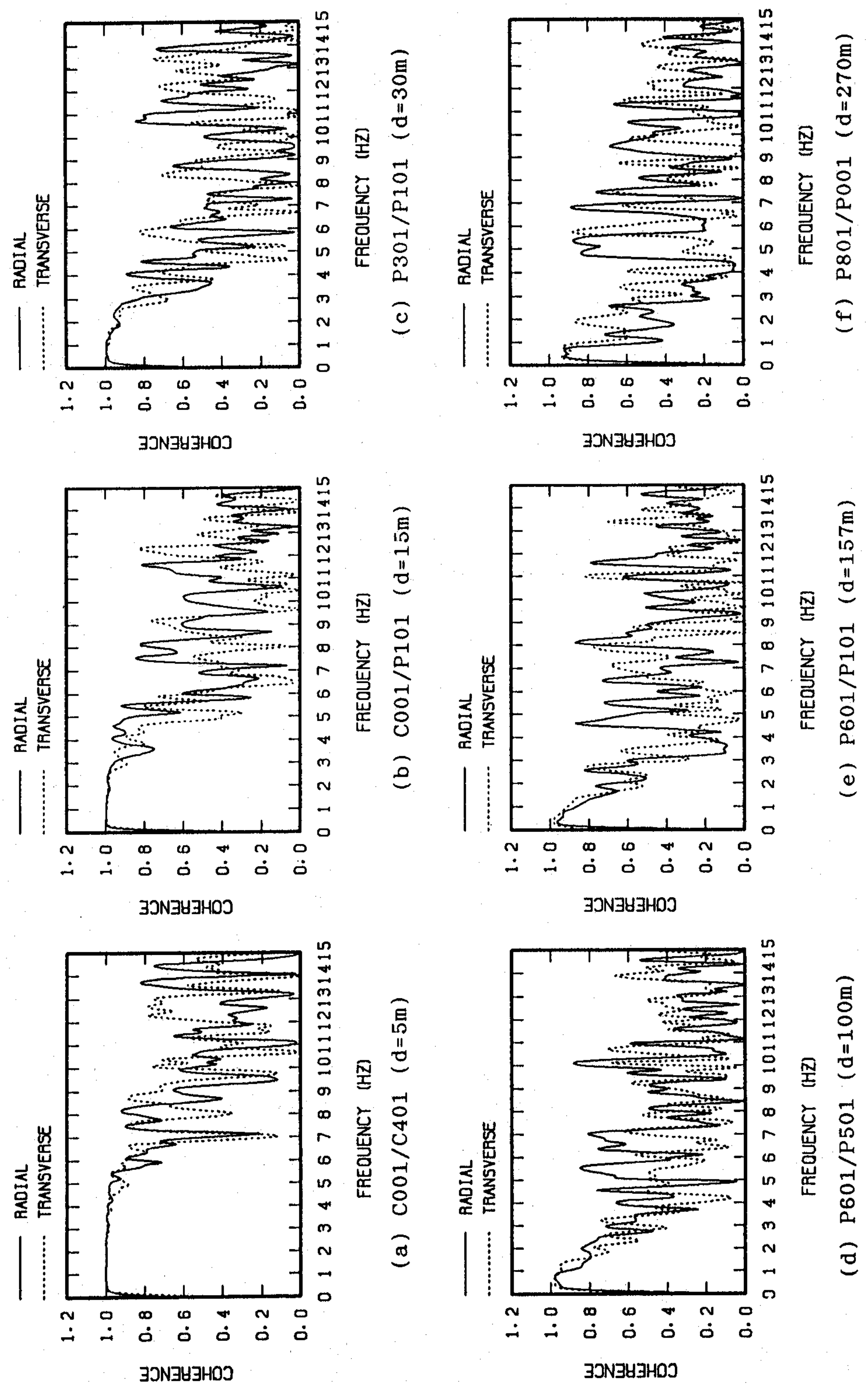

Figure 9. Coherence functions calculated from records of the Tokyo-Tobu earthquake for t = 12–24 s

coherence generally decreases with the larger separation distance and the higher frequency. Hence it may be reasonable to model the coherence as a function $\mathrm{coh}^2(f, \mathbf{d})$ of frequency and separation vector.[22] No large difference can be seen between the coherence functions for the radial and transverse components. The coherence functions for the UD-component were also calculated for the initial P-wave part (0–12 s) of time series, although they are not shown here. The coherence functions for the UD-component were found to be larger than those for the horizontal components, especially in the high frequency range. More comprehensive studies may be required, in which various combinations of two points and various earthquake events are investigated, to obtain rational analytical coherence models.

SOIL AMPLIFICATION DURING THE CHIBAKEN TOHO-OKI EARTHQUAKE

As the second example of the database, the Chibaken-Toho-Oki earthquake (IEQK = 8722) was used to demonstrate soil amplification of the site. First, by the tripartite method, the incident seismic wave to the site was confirmed to be almost vertically propagating. Then the soil amplification from the recorded motions is compared with those by one-dimensional earthquake response analyses. Two analysis methods, the equivalent linear technique in the program SHAKE[23] and the step-by-step non-linear response analysis, are employed.

The layered soil model was constructed as shown in Table III based on the geological exploration. In this table, the unit weight and non-linear soil parameters were assumed from the authors' experience because no test data are available in the Chiba Station. In order to represent the non-linear relationship between the shear strain and the shear stress, the Ramberg–Osgood (RO) model is employed with the skeleton curve

Table III. Soil modelling of the Chiba array site

Layer No.	Soil Type	Depth G.L. (m)	Sub-Layer	Location of Accelero-meters	V_s (m/s)	V_p (m/s)	Unit Weight* γ_t (t/m^3)	Initial Damping Ratio* (h_0)	Maximum Damping Ratio* (h_{max})	Reference Strain* (γ_r)
1	Loam	0.0 / ▽ -5.0		GL-1 / GL-5	140	320	1.15	0.02	0.25	3×10^{-3}
2	Sandy Clay	▽ -10.0		GL-10	320	550	1.50	0.02	0.25	3×10^{-3}
3	Fine Sand	▽ -15.0			320	550	1.95	0.02	0.25	5×10^{-4}
4		▽ -24.0		GL-20	320	1670	1.95	0.02	0.25	8×10^{-4}
5		▽ -40.0		GL-40	420	1670	2.00	0.02	0.25	8×10^{-4}

* assumed

expressed as follows:

$$\tau = \frac{G_0 \gamma}{1 + \alpha |\tau|^\beta} \tag{2}$$

where τ is the shear stress, γ is the shear strain, G_0 is the initial shear modulus, and α and β are the parameters of the RO model. These two parameters are determined as[24]

$$\alpha = \left(\frac{2}{\gamma_r G_0}\right)^\beta; \qquad \beta = \frac{2\pi h_{max}}{2 - \pi h_{max}} \tag{3}$$

where γ_r is the shear strain when the shear modulus G reduces to 1/2 of its initial value ($G/G_0 = 0{\cdot}5$), and h_{max} is the damping ratio when the shear strain goes to infinity. From equation (2), G/G_0 is written as

$$G/G_0 = \frac{1}{1 + \alpha |\tau|^\beta} \tag{4}$$

The relationship between G/G_0 and γ can be constructed numerically based on equations (2) and (4).

Introducing the Masing rule, the damping ratio h is evaluated by the area of the hysteresis loop. The initial linear damping ratio h_0 is added in this study to avoid an infinitesimal value of h for the very small strain level. Thus the damping ratio for this RO model is described as

$$h = h_{max}(1 - G/G_0) + h_0 \tag{5}$$

In the non-linear response analysis, this h_0 is considered as the Rayleigh damping for the first two modes of the linear system. Figure 10 plots the non-linear soil properties used in the analyses.

The response analyses were performed for the NS-component of the Chibaken-Toho-Oki earthquake. The 0–36 s of the recorded motion at C040 (GL − 40 m of the borehole C0) was employed as an input motion. The conditions of the equivalent linear analysis were determined as follows: the time interval $\Delta t = 0{\cdot}005$ s; the number of data points for the Fast Fourier Transform (FFT) $N = 8192$; the cutoff frequency $f_{max} = 20$ Hz; the effective shear strain factor 0·7; and the allowable error for convergence = 5 per cent. In the non-linear analysis, the time integration was carried out by using the Newmark β method.

The maximum response values obtained by these two analyses are shown in Figure 11. The peak ground accelerations by the analyses are in good agreement with the recorded ones. The maximum shear strains are smaller than 0·1 per cent, thus the responses by the equivalent linear method and the non-linear method are very close. Note that, in this figure, G/G_0 and the damping ratio for the RO model correspond to the

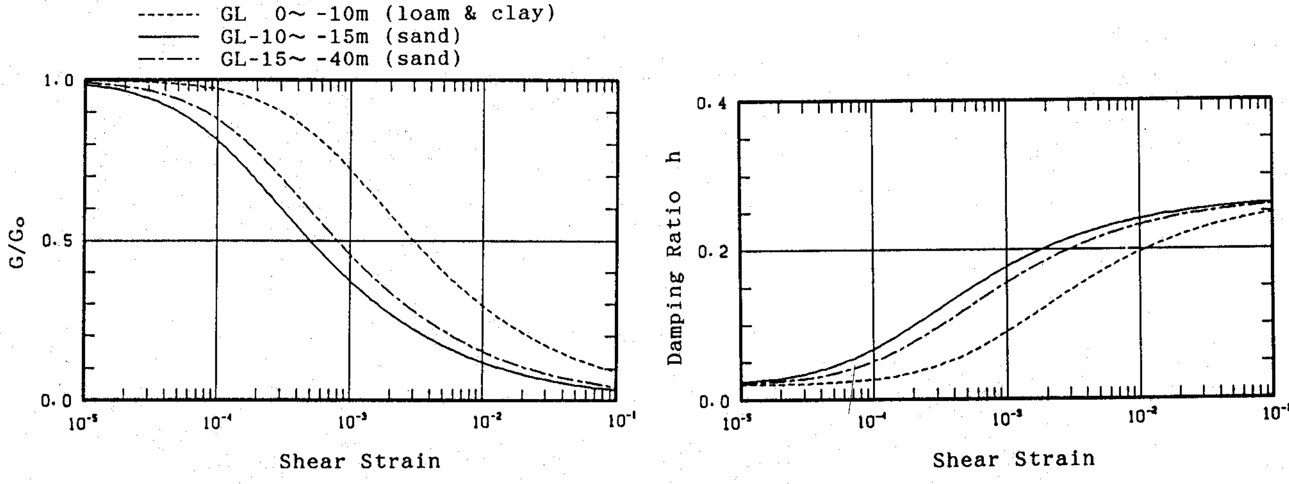

Figure 10. Strain-dependent soil properties used for response analyses

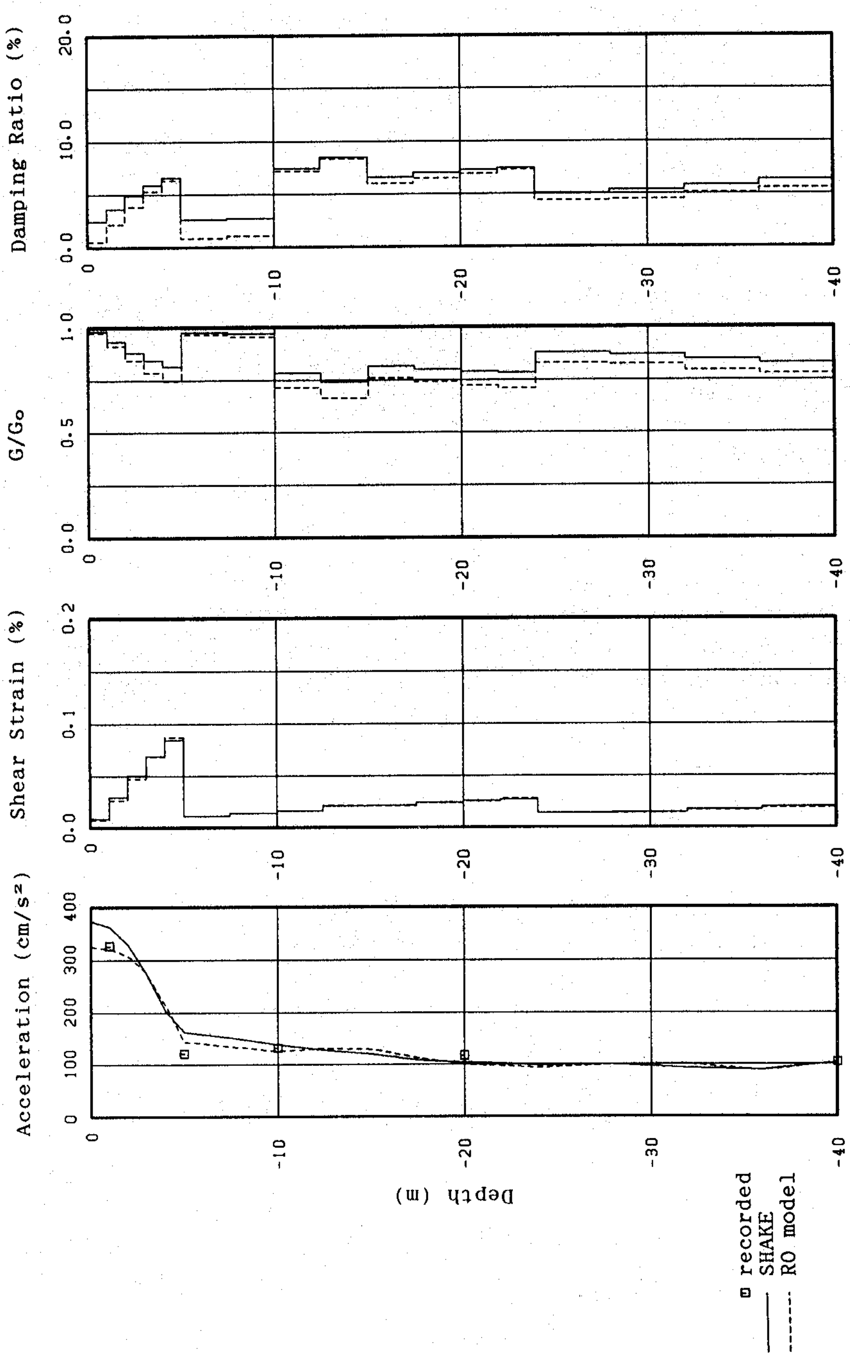

Figure 11. Computed maximum response values for NS-component of the Chibaken-Toho-Oki earthquake

maximum shear strain, while those from SHAKE correspond to the effective shear strain. The computed acceleration time histories by the non-linear analysis are compared with the recorded ones in Figure 12. The agreement between them is found to be satisfactory. The analysis by SHAKE also gave similar time histories to the recorded ones, although they are not shown here.

More detailed comparison is made between the recorded and computed ground motions in terms of the transfer function

$$H_{xy}(f) = S_{xy}(f)/S_{xx}(f) \tag{6}$$

and the coherence function $\mathrm{coh}^2(f)$. In evaluating the power and cross spectra, the Parzen window is again employed with the band width of 0·4 Hz. In the case of analysis by SHAKE, the transfer function is evaluated analytically. However, in order to obtain comparable smoothing effect with those of the recorded motions and the non-linear analysis results, the transfer function for SHAKE was also calculated from the time histories.

Figure 13 shows the absolute values of the transfer functions (C001/C020, C001/C040) for the recorded motions and the results of two analysis methods. Although the transfer functions for the recorded motions show smaller amplitude at the first natural frequency, their overall agreement is fairly good.

The corresponding coherence functions are depicted in Figure 13. Both those from the non-linear analysis and from the recorded motions decrease as the frequency becomes large, while those from SHAKE decrease only around the natural frequencies. Three reasons are considered for the reduction of coherence in this situation:

(i) the effect of smoothing at the natural frequencies;
(ii) the effect of non-linearity of the system;
(iii) the effect of random incident angles of the input motion. Only reason (i) is considered for the equivalent linear analysis (SHAKE), (i) and (ii) are involved for the non-linear analysis (RO model), and all three reasons may be included for the recorded motions. The difference of three lines in the figure may be

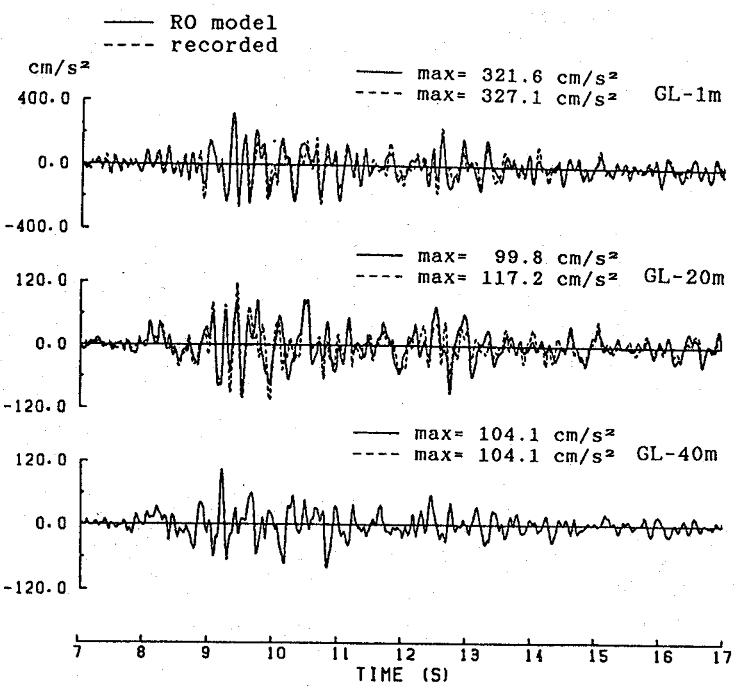

Figure 12. Comparison of recorded and computed ground motions for NS-component of the Chibaken-Toho-Oki earthquake

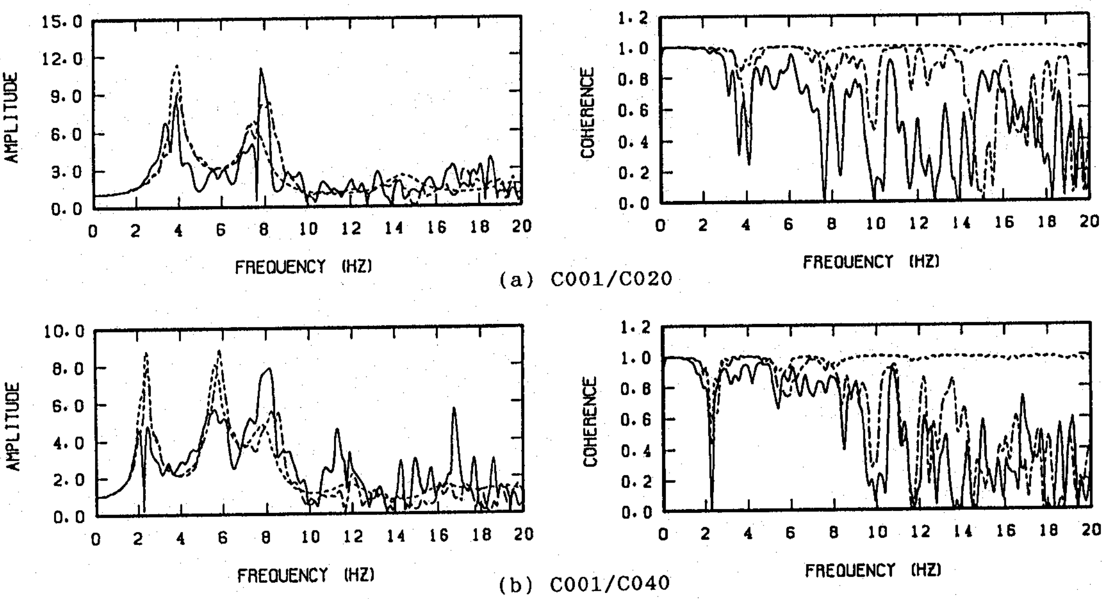

Figure 13. Transfer functions (left) and coherence functions (right) of recorded and computed ground motions for NS-component of the Chibaken-Toho-Oki earthquake

explained by these reasons. The drops of the transfer function from the records at the natural frequencies can also be attributed to the reduction of the corresponding coherence function.

CONCLUSIONS

A strong motion database is developed for a dense seismometer array in the Chiba Experiment Station. The array system consists of a three-dimensional arrangement of borehole accelerometers and a complementary observation system for pipe and ground strains. The system has been operating successfully since 1982 and more than 160 events have been recorded. In order to utilize these valuable data effectively, a database comprising 27 major events has recently been created.

Because of the dense arrangement of seismometers, the recorded motions may be especially useful when evaluating the spatial correlation characteristics of seismic waves. Using a typical event in the database, the spatial variation of ground motion was examined with the aid of principal axes and the coherence functions. The soil amplification is another important issue for the Chiba array. The transfer functions calculated from the records were well explained by the equivalent linear and the non-linear analyses.

The Chiba array database is available from the authors by request.

ACKNOWLEDGEMENT

The authors express their appreciation to the Ministry of Education, Science and Culture of Japanese Government, Fujita Corporation and Kubota for their financial support to the array installation. Special thanks are extended to Mr Nobuhiko Sato of Tokyo Sokushin Co., Ltd., formerly a research associate of University of Tokyo, for his continuing efforts for the development and operation of the Chiba array system.

REFERENCES

1. B. A. Bolt, Y. B. Tsai, K. Yeh and M. K. Hsu, 'Earthquake strong motions recorded by a large near-source array of digital seismographs', *Earthquake eng. struct. dyn.* **10**, 561–573 (1982).
2. C. H. Loh, J. Penzien and Y. B. Tsai, 'Engineering analysis of SMART 1 array accelerograms', *Earthquake eng. struct. dyn.* **10**, 575–591 (1982).

3. T. Harada and T. Oda, 'Probabilistic modeling of spatial variation of seismic ground deformation', *Proc. 4th int. conf. struct. safety reliability* **II**, 277–286 (1985).
4. R. Harichandran and E. H. Vanmarcke, 'Stochastic variation of earthquake ground motion in space and time', *J. eng. mech. ASCE* **112**, 154–174 (1986).
5. N. Abrahamson, 'Spatial interpolation of array ground motions for engineering analysis', *Proc. 9th world conf. earthquake eng.*, Tokyo-Kyoto **II**, 227–232 (1988).
6. T. Ishii, T. Sato and T. Satoh, 'A study on seismic wave propagation in Lotung, Taiwan', *Trans. 10th int. conf. struct. mech. reactor technol.* **K1**, 7–12 (1989).
7. S. Omote *et al.* 'Observation of earthquake strong-motion with deep boreholes—An introductory note for Iwaki and Tomioka Observation Station in Japan', *Proc. 8th world conf. earthquake eng.*, San Francisco **II**, 247–254 (1984).
8. Y. Kitagawa, I. Ohkawa and T. Kashima, 'Dense strong motion earthquake seismometer array at site with different topographic and geologic conditions in Sendai', *Proc. 9th world conf. earthquake eng.*, Tokyo-Kyoto **II**, 215–220 (1988).
9. T. Tazoh, M. Sato, K. Shimizu and A. Hatakeyama, 'Nonlinear seismic response analysis of soil deposit using strong seismic records', *Proc. 9th world conf. earthquake eng.*, Tokyo-Kyoto **II**, 507–512 (1988).
10. T. Katayama and N. Sato, 'Ground strain measurement by a very densely located seismometer array', *Proc. 6th Japan earthquake eng. symp.* 241–248 (1982).
11. T. Katayama, J. Farjoodi and N. Sato, 'Measurement of seismic ground strain by a dense seismometer array', *Proc. 8th world conf. earthquake eng.*, San Francisco **II**, 207–214 (1984).
12. J. Farjoodi and T. Katayama, 'Application of dense seismograph array data to evaluate engineering properties of strong ground motions', *Proc. 7th Japan earthquake eng. symp.* 511–516 (1986).
13. N. Sato, T. Katayama, M. Nakamura, T. Iwamoto and N. Ohbo, 'Observation of seismic ground motion and buried pipe strain in a very dense seismometer array', *Proc. 9th world conf. earthquake eng.*, Tokyo-Kyoto **VII**, 29–34 (1988).
14. H. T. Tang *et al.* 'A large-scale soil–structure interaction experiment: Design and construction', *Nucl. eng. des.* **111**, 371–379 (1989).
15. S. Noda, E. Kurata and H. Tsuchida, 'Observation of earthquake motions by dense instrument arrays at soft ground', *Proc. 9th world conf. earthquake eng.*, Tokyo-Kyoto **II**, 221–226 (1988).
16. T. Okubo, T. Arakawa and K. Kawashima, 'Dense instrument array program of the Public Works Research Institute and preliminary analysis of the records', *Proc. 8th world conf. earthquake eng.*, San Francisco **II**, 151–158 (1984).
17. J. F. Lander, C. A. Angel and J. L. Coffman, 'Activities of the World Data Center in Earthquake Engineering', *Proc. 8th world conf. earthquake eng.*, San Francisco **II**, 79–86 (1984).
18. Working Group for Strong Motion Arrays, 'Research report on development of a database for strong motion array records—Introduction of array observation systems in Japan and prospect for a cooperative database system', Earthquake Engineering Committee, JSCE, 1989.
19. I. Muramatsu, 'Development of velocity seismograph', (in Japanese) *Jishin* **30**, 317–338 (1977).
20. J. Penzien and M. Watabe, 'Characteristics of 3-dimensional earthquake ground motions', *Earthquake eng. struct. dyn.* **3**, 365–373 (1975).
21. T. Kubo and J. Penzien, 'Analysis of three-dimensional strong motions along principal axes, San Fernando earthquake', *Earthquake eng. struct. dyn.* **7**, 265–278 (1979).
22. C. H. Loh, 'Analysis of the spatial variation of seismic waves and ground movements from SMART-1 array data', *Earthquake eng. struct. dyn.* **13**, 561–581 (1985).
23. P. B. Schnabel, J. Lysmer and H. B. Seed, 'SHAKE—A computer program for earthquake response analysis of horizontally layered sites', *Report No. EERC 72-12*, Earthquake Engineering Research Center, University of California, Berkeley, CA, 1972.
24. F. Tatsuoka and S. Fukushima, 'Stress–strain relation of sand for irregular cyclic excitation (1)' (in Japanese), *Seisan-kenkyu* **30**, No. 9, (1978).